

The SCF^{Slmb} ubiquitin ligase regulates Plk4/Sak levels to block centriole reduplication

Gregory C. Rogers,¹ Nasser M. Rusan,¹ David M. Roberts,^{1,3} Mark Peifer,^{1,3} and Stephen L. Rogers^{1,2,3}

¹Department of Biology, ²Carolina Center for Genome Sciences, and ³Lineberger Comprehensive Cancer Center, University of North Carolina at Chapel Hill, Chapel Hill, NC 27599

Restricting centriole duplication to once per cell cycle is critical for chromosome segregation and genomic stability, but the mechanisms underlying this block to reduplication are unclear. Genetic analyses have suggested an involvement for Skp/Cullin/F box (SCF)-class ubiquitin ligases in this process. In this study, we describe a mechanism to prevent centriole reduplication in *Drosophila melanogaster* whereby the SCF E3 ubiquitin ligase in complex with the F-box protein Slmb mediates proteolytic degradation of the centrosomal

regulatory kinase Plk4. We identified SCF^{Slmb} as a regulator of centriole duplication via an RNA interference (RNAi) screen of Cullin-based ubiquitin ligases. We found that Plk4 binds to Slmb and is an SCF^{Slmb} target. Both Slmb and Plk4 localize to centrioles, with Plk4 levels highest at mitosis and absent during S phase. Using a Plk4 Slmb-binding mutant and Slmb RNAi, we show that Slmb regulates Plk4 localization to centrioles during interphase, thus regulating centriole number and ensuring the block to centriole reduplication.

Introduction

Centrosomes play fundamental roles in regulating chromosome segregation and the interphase microtubule cytoskeleton. Animal cells enter mitosis with two centrosomes, which assemble a bipolar spindle to facilitate chromosome segregation. Centrosomes assemble from centrioles that, like DNA, are duplicated once and only once per cell cycle (Fig. S1 A, available at <http://www.jcb.org/cgi/content/full/jcb.200808049/DC1>; Wong and Stearns, 2003). Errors in centriole duplication lead to cells with too many or too few centrosomes; the resulting monopolar or multipolar spindles disrupt chromosome segregation and can lead to genomic instability (Brinkley, 2001). Interestingly, there is a correlation between excess centrosomes, aneuploidy, and cancer (Nigg, 2006), but which is the cause or consequence is unclear. Thus, understanding regulatory mechanisms governing centrosome duplication may provide insights into both normal cell behavior and tumorigenesis.

To prevent centriole overduplication, eukaryotic cells possess a robust mechanism that blocks reduplication (Hinchcliffe et al., 1998; Wong and Stearns, 2003; Tsou and Stearns, 2006a). The mechanism preventing centriole reduplication remains un-

clear, but analogies to DNA replication may provide insight. During S phase, several mechanisms prevent DNA rereplication (Blow and Dutta, 2005). One utilizes Cullin-based E3 ubiquitin ligases, which control the specificity and timing of protein degradation by tagging substrates with ubiquitin, targeting them for proteasomal proteolysis (Deshaies, 1999). During DNA replication, E3 ubiquitin ligases mediate the destruction of replication-initiation factors to prevent origin refiring (DePamphilis et al., 2006). Thus, we thus explored whether centriole replication might be similarly controlled by E3 ubiquitin ligases.

The best characterized Cullin-based E3 ligases are the Skp/Cullin/F box (SCF) family (Deshaies, 1999). SCF ligases are a complex of four subunits (Roc–Cullin–Skp–F box), each encoded by a multigene family. A Roc–Cullin–Skp complex forms the ubiquitin ligase core, whereas F-box proteins are interchangeable substrate-binding subunits that dictate substrate specificity. Interestingly, genetic studies in *Drosophila melanogaster* and mice revealed that mutations in SCF components, including *Drosophila skpA* or the F-box genes *slmb* or *skp2*, all lead to supernumerary centrosomes (Nakayama et al., 2000; Wojcik et al., 2000; Guardavaccaro et al., 2003; Murphy, 2003). Furthermore, mammalian Skp1 and Cul1 localize to centrosomes

N.M. Rusan and D.M. Roberts contributed equally to this paper.

Correspondence to Stephen L. Rogers: srogers@bio.unc.edu

Abbreviations used in this paper: CLB, cell lysis buffer; D-PLP, *Drosophila* pericentrin-like protein; dsRNA, double-stranded RNA; HTM, high-throughput microscopy; HU, hydroxyurea; Nlp, nucleophosmin; PCM, pericentriolar material; SAS-6p, SAS-6 promoter; SBM, Slmb-binding mutant; SCF, Skp/Cullin/F box.

© 2009 Rogers et al. This article is distributed under the terms of an Attribution-Noncommercial-Share Alike-No Mirror Sites license for the first six months after the publication date (see <http://www.jcb.org/misc/terms.shtml>). After six months it is available under a Creative Commons License (Attribution-Noncommercial-Share Alike 3.0 Unported license, as described at <http://creativecommons.org/licenses/by-nc-sa/3.0/>).

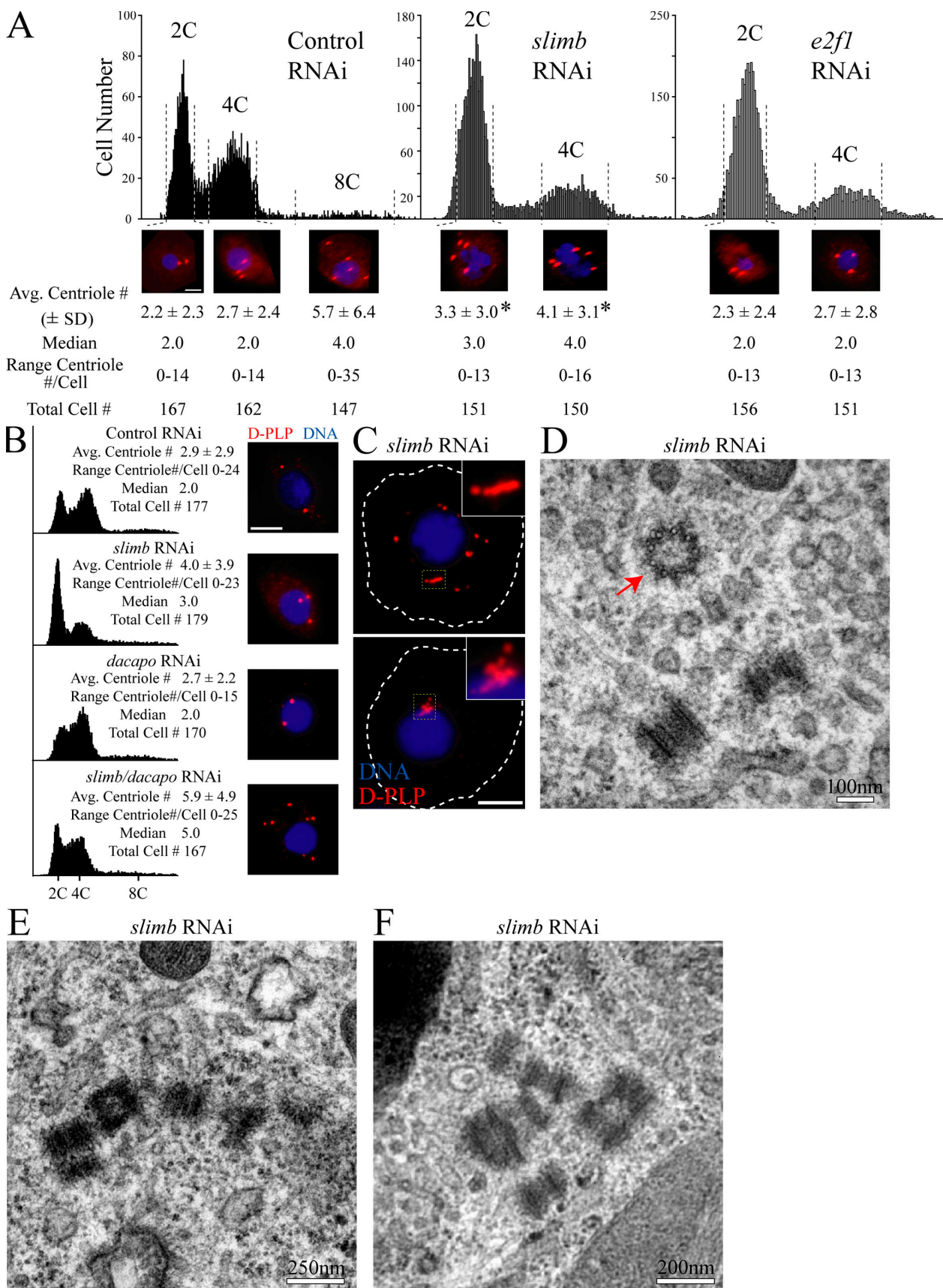


Figure 1. *slimb* RNAi elevates centriole number. (A) Effects of *slimb* RNAi are not solely via effects on cell cycle. Cells stained for D-PLP (red) and DNA (blue) were quantitated for DNA content by HTM (5,000 cells/histogram). Centrioles were manually counted in ~150 randomly selected cells with 2C, 4C, or 8C DNA. Example cells and mean, median, and range of centriole numbers are shown below sampled histogram regions. Histograms are not

(Freed et al., 1999), and chemical inhibition of proteasomes promotes abnormal centriole overduplication in human cells (Duensing et al., 2007). These data implicate at least two complexes (SCF^{Slimb} and SCF^{Skp2}) in regulating centrosome duplication, but the identity of the target involved remains unknown. In this study, we report that SCF^{Slimb} regulates centriole duplication by targeting the key centrosomal regulator Plk4 for proteolytic degradation, thus contributing to the centrosome reduplication block.

Results

An RNAi screen for Cullin-based ligases that limit centriole duplication identifies SCF^{Slimb}

We examined roles of Cullin-based ubiquitin ligases in centriole duplication using functional genomics in cultured *Drosophila* S2 cells. We identified all members of the Roc–Cullin–Skp–F-box gene families in *Drosophila*, revealing 3 Roc (Noureddine et al., 2002), 6 Cullin, 7 Skp, and 42 F-box genes. We used RNAi to deplete each protein (when antibodies were available, we confirmed RNAi depletion by immunoblotting; Fig. S1 B) and applied two sequential functional screens to measure changes in centrosome or centriole number. In the first screen, we counted γ -tubulin–labeled centrosomes in mitotic cells. 4 of 58 genes scored positive: *skpA*, *skpB*, *slimb*, or *skp2* RNAi increased centrosome number (Table S1, available at <http://www.jcb.org/cgi/content/full/jcb.200808049/DC1>). All other RNAi treatments yielded wild-type centrosome numbers; none decreased centrosome number. However, the RNAi of some SCF subunits (*Roc1a*, *cul-1*, and *rca1*) induced interphase arrest, as SCF regulates cell cycle progression (Vodermaier, 2004), preventing assessment of their roles. To circumvent this and verify positives from the first screen, we used a second screen to measure changes in interphase centriole number by immunostaining for the centriole protein *Drosophila* pericentrin-like protein (D-PLP; Fig. S1 C; Martinez-Campos et al., 2004). D-PLP is not only a centriolar protein but also a component of the pericentriolar material (PCM; Martinez-Campos et al., 2004); however, centrioles in interphase S2 cells do not recruit PCM, nor do they nucleate microtubule growth (Rogers et al., 2008). Thus, D-PLP marks centrioles in these cells. In this assay, only depletion of the canonical SCF core subunits *Roc1a/Cul-1/SkpA* and the F-box protein *Slimb* elevated both mean and median number of D-PLP spots. We note that control cells possess a higher than expected mean mitotic centrosome number (3.2 ± 3.0 ; range of 0–36 per cell) and interphase centriole number (3.1 ± 3.0 ; range of 0–25 per cell). This is partially caused by a fraction ($\sim 10\%$) of polyploid cells that apparently spontaneously arise in an S2 cell population and contain numerous centrioles (Fig. 1 A). In spite of this, many cells (45%) contain two D-PLP spots (Fig. S2 B).

We confirmed the increased centriole number using EGFP–SAS-6 as a centriole marker; median centriole number increased by one after *Slimb* depletion ($n = 194$ cells examined). *Slimb* depletion also increased multipolar spindle frequency (Fig. S1 D), which is consistent with increased centrosome number. These data suggest that no single Cullin or identifiable Cullin-based ubiquitin ligase component is essential for centriole duplication in S2 cells and that SCF^{Slimb} suppresses centriole overduplication. Furthermore, these data are consistent with previously published work implicating *Slimb*/ β -Trcp1 and *SkpA* in regulating centrosome number in *Drosophila* and mammalian cells (Wojcik et al., 2000; Guardavaccaro et al., 2003; Murphy, 2003).

Slimb plays a separate role in cell cycle progression, limiting the extent of centriole overduplication

Because *Slimb* has been implicated in cell cycle progression (Wojcik et al., 2000), we examined whether elevated centriole number was simply an indirect consequence of altering the cell cycle. *Drosophila* centrioles, like their counterparts in mammalian cells, duplicate during S phase and disengage during telophase (Fig. S2 A). The centriole markers available in *Drosophila* do not allow us to resolve centriole singlets from pairs because of their close association after duplication. Thus, we used D-PLP to mark centrioles, with the caveat that a D-PLP spot could represent either a centriole singlet or a doublet before disengagement. To test whether cell cycle alterations caused the differences in apparent centriole number we observed in *slimb* mutants, we developed a high-throughput microscopy (HTM) assay to simultaneously quantitate DNA and centriole number. RNAi-treated cells were stained with DAPI and anti-D-PLP and scanned by HTM to measure DNA content, thus assessing centriole number at each cell cycle stage (Fig. 1 A and Fig. S2 C). Wild-type cells with either 2C (G1 phase) or 4C (G2 and M phases) DNA content had similar centriole numbers because we cannot distinguish the centriole singlets and doublets present at these respective cell cycle phases.

Strikingly, *Slimb* depletion elevated centriole numbers in both 2C (G1 phase) and 4C (G2 and M phases) populations (Fig. 1 A). However, it also increased the fraction of G1-phase (2C) cells. Because *Slimb* depletion affects both centriole number and causes G1 arrest, we tested whether increased centriole number is solely an indirect effect of increasing the fraction of G1-phase cells. This was not the case, as RNAi of E2F1, a transcription factor required for G1 to S-phase progression (Dimova et al., 2003), also increased G1-phase cells without elevating centriole number (Fig. 1 A).

Cdk2–cyclin E activity is high during S phase, when it is required for centriole duplication (Winey, 1999), and low during G1 phase, limiting G1 centriole duplication. We hypothesized

shown to scale. Asterisks denote a significant difference; *, $P < 0.007$ (unpaired *t* test). *Slimb* or E2F1 depletion eliminates the 8C population. (B) Cell cycle progression (assessed via HTM; 5,000 cells/histogram) and centriole number were scored in day 7 RNAi-treated cells. D-PLP–labeled centrioles (red) were manually counted. Histograms are shown to scale. (C) Unique centriole configurations in *Slimb*-depleted cells that contained more than the mean number of D-PLP–labeled centrioles (red). White tracing marks cell borders. Insets show centrioles at a higher magnification. (A–C) Bars, 5 μ m. (D–F) Transmission electron micrographs of interphase *Slimb*-depleted cells. (D) Typical centriolar microtubule arrangement of the centriole in cross section (red arrow). Other centrioles are sagittal sections oriented in different manners. Excess centrioles in rows (E) and clusters (F).

that *slimb* RNAi-mediated G1 arrest may limit the cell's capacity to produce more centrioles, thus underestimating Slimb's role in restricting centriole reduplication. To fully uncover Slimb's role, we bypassed the putative G1 arrest by simultaneously depleting the cyclin-dependent kinase inhibitor Dacapo that establishes G1 phase in *Drosophila* (de Nooij et al., 1996; Lane et al., 1996). *dacapo* RNAi alone did not appreciably alter cell cycle distribution or centriole number (Fig. 1 B and Fig. S1 C). However, codepleting Slimb and Dacapo alleviated the G1 arrest caused by *slimb* RNAi alone and restored cell cycle progression (Fig. 1 B). Strikingly, it also further increased centriole number compared with *slimb* RNAi alone (Fig. 1 B and Fig. S1 C), suggesting that Slimb plays separate roles in limiting centriole duplication and in cell cycle progression.

These data are consistent with two different possible effects of Slimb depletion. First, Slimb might normally restrain centriole duplication to once per cell cycle. Second, Slimb depletion might lead to premature centriole disengagement; because we cannot distinguish centriole singlets and doublets using light microscopy, this would create the appearance of more centrioles. To determine whether the increase in D-PLP spots represents overduplication of bona fide centrioles, we examined centriole morphology in Slimb-depleted cells by both light microscopy and EM. By EM, centrioles in Slimb-depleted cells had the characteristic cylindrical shape with nine doublet microtubules (Fig. 1 D). This suggests that the steps of centriole duplication most likely occur normally. However, Slimb-depleted cells differed from wild type in another significant way. In wild type, 28 of 29 centrioles imaged by EM were normal singlets or doublets. In contrast, in Slimb-depleted cells, six of nine centrioles imaged by EM had multiple centrioles in clusters, which is inconsistent with either a normal singlet or doublet. Mutant cells that contained more than a mean number of centrioles had these centrioles arranged in discrete centriole chains or clusters, which could be visualized either at the EM or light levels (at the light level, 30% of Slimb-depleted cells had interphase centriole clusters [$n = 98$], whereas no control cells had these [$n = 100$]; Fig. 1, C, E, and F). Together, these data suggest that the putative Slimb target is likely a key regulator of centriole duplication, which is consistent with earlier work *in vivo* that also supported a role in centriole duplication and not simply in disengagement (Wojcik et al., 2000).

Slimb localizes to centrioles

We hypothesized that if Slimb regulates centriole duplication, it might localize to centrioles. To test this, we generated antisera specifically recognizing Slimb (Fig. 2, A and B). Although mostly cytoplasmic, Slimb was enriched on D-PLP-labeled centrioles in interphase S2 cells (Fig. 2 C). In contrast, Slimb immunostaining at centrioles was significantly reduced by Slimb depletion (Fig. S2 D). To confirm this localization, we examined an S2 stable line expressing both Slimb-EGFP and mCherry-SAS-6 (a centriole protein; Rusan and Peifer, 2007). Like Slimb, Slimb-EGFP was enriched at mCherry-SAS-6-labeled centrioles in live interphase cells (Fig. 2 D). Furthermore, a fraction of both endogenous and EGFP-tagged Slimb copurified with centrioles isolated using sucrose gradient centrifugation (Fig. 2 F). These data demonstrate that Slimb associates with centrioles. In addition, we noted that Slimb occasionally appeared asymmetrically positioned on centrioles in live cells (Fig. 2 D and Video 1, available at <http://www.jcb.org/cgi/content/full/jcb.200808049/DC1>). However, centrioles in these cells are not stationary but instead constantly spin and move apparently randomly throughout the cell (Rogers et al., 2008). Thus, this perceived asymmetry in Slimb localization on centrioles is likely the result of a delay in image acquisition using live cell microscopy.

Next, we examined Slimb localization to centrioles during specific cell cycle phases, as centriole duplication is an event tightly coupled to cell cycle progression (Fig. 2 F). Thus, we chemically arrested cells during S, G2, and M phases and examined Slimb protein levels and centriole localization. Strikingly, Slimb immunostaining to centrioles was apparently not cell cycle regulated, as Slimb localized to centrioles during these cell cycle stages (Fig. 2 F). Similarly, quantitative immunoblots revealed that total Slimb levels are relatively high throughout these phases, peaking during G2 and remaining elevated during mitosis (Fig. 2 G). Thus, Slimb associates with centrioles during all of the cell cycle phases that we examined.

The tumor suppressor Plk4 is a target for Slimb-mediated ubiquitination

We hypothesized that SCF^{Slimb} depletion stabilizes a central regulator of centriole duplication, promoting overduplication. The kinase Plk4 (also called Sak), a tumor suppressor (Ko et al., 2005), is essential for centriole duplication, and Plk4 overexpression produces supernumerary centrioles (Bettencourt-Dias et al., 2005; Habedanck et al., 2005; Kleylein-Sohn et al., 2007; Peel et al., 2007; Rodrigues-Martins et al., 2007). Thus, we explored whether Plk4 is an SCF^{Slimb} target. Consistent with this hypothesis, we identified a potential Slimb-binding site on *Drosophila* Plk4 downstream of the kinase domain; this sequence (DSGIIT) fits the Slimb-binding consensus (DpSGXXp[S/T]) and is conserved in vertebrate Plk4 orthologues (Fig. 3 A).

As a first test of the hypothesis that Plk4 is a Slimb target, we examined whether Slimb coimmunoprecipitated with Plk4 from a stable S2 cell line expressing Plk4-myc. Affinity-purified anti-Slimb antibodies, but not preimmune antisera, immunoprecipitated endogenous Slimb and coimmunoprecipitated the SCF protein SkpA and Plk4-myc (Fig. 3 B). Likewise, in the reciprocal experiment, anti-GFP antibody coimmunoprecipitated endogenous Slimb from cells expressing Plk4-EGFP (Fig. 3 C, left). Thus, Plk4 associates with Slimb.

The putative Slimb-binding consensus in Plk4 suggests that Plk4 could directly bind Slimb and be a ubiquitination substrate (Fig. 3 A). To test this, we generated a Slimb-binding mutant (SBM) of Plk4 (Plk4-SBM-EGFP), mutating two key residues in the binding consensus, changing DSGIIT to DAGIIT (S293A/T297A). Phosphorylation of these serine and threonine residues is typically required for Slimb recognition and ubiquitination (Smelkinson and Kalderon, 2006). Anti-GFP antibody immunoprecipitated Plk4-SBM-EGFP but did not coimmunoprecipitate endogenous Slimb (Fig. 3 C, right). Furthermore, when coexpressed with triple Flag-tagged fly ubiquitin,

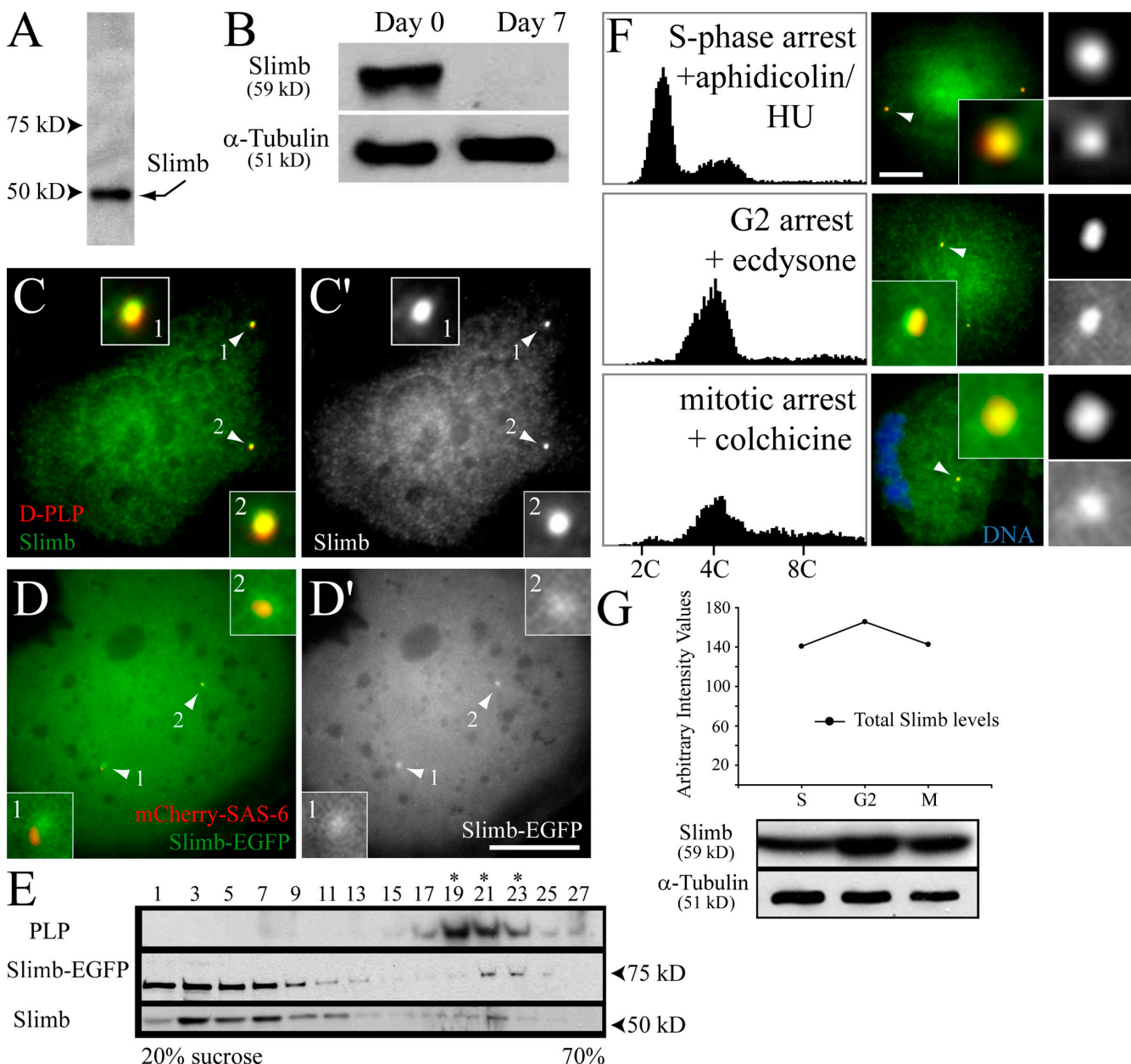


Figure 2. Slimb localizes to centrioles. (A) Immunoblot of affinity-purified anti-Slimb antibody against an S2 cell lysate. (B) *slimb* RNAi depletes protein by 98%. (C and C') Immunostaining of Slimb (green, monochrome) and D-PLP centrioles (red) in interphase S2 cells. (D and D') Stable S2 line expressing Slimb-EGFP (green, monochrome) and mCherry-SAS-6 centrioles in live interphase cells. (C–D') Centrioles (arrowheads) are shown at a higher magnification (insets). (E) Endogenous Slimb and Slimb-EGFP cosediment with centrioles purified from S2 cells on a 20–70% sucrose gradient. Fractions were immunoblotted for D-PLP, GFP, and Slimb. Asterisks denote peak centriole-containing fractions. (F) Slimb (green, arrowheads) immunolocalizes to D-PLP centrioles (red) after 24-h drug-induced S, G2, or M-phase arrest. Histograms (to scale) of DNA content assessed by HTM (5,000 cells/histogram). Condensed DNA (blue) reveals a mitotic cell. Insets show centrioles at a higher magnification. (G) Graph of endogenous Slimb levels after 24-h drug-induced cell cycle arrest as determined from quantitative anti-Slimb immunoblots (below graph). (B and G) α-Tubulin was used as a loading control. Bars, 5 μm.

immunoprecipitated Plk4-EGFP was labeled with Flag-ubiquitin, whereas Plk4-SBM-EGFP was not (Fig. 3 D). These data suggest that association and ubiquitination occurs via a phosphorylated Slimb-binding domain in Plk4.

If Plk4 is a Slimb target, Slimb depletion should stabilize Plk4. To assess this, we generated an S2 stable line expressing Plk4-EGFP and measured Plk4 levels by immunoblotting for GFP after depleting different F-box proteins. Whereas Plk4-EGFP levels were extremely low in control or cells depleted of the F-box proteins Skp2 or Ago, Plk4-EGFP accumulated after

slimb RNAi (Fig. 3 E and Fig. S3 A, available at <http://www.jcb.org/cgi/content/full/jcb.200808049/DC1>). Thus, Slimb normally down-regulates Plk4 levels.

Because mutation of two putatively phosphorylated residues within the Slimb-binding consensus abolished both Slimb binding and ubiquitination, we next examined the phosphorylation state of Plk4 in cells containing or depleted of Slimb. Plk4-EGFP expressed in control cells migrates as an ~110-kD polypeptide (Fig. 3 F, left). Markedly, Slimb depletion led to the appearance of an abundant slower migrating species of Plk4

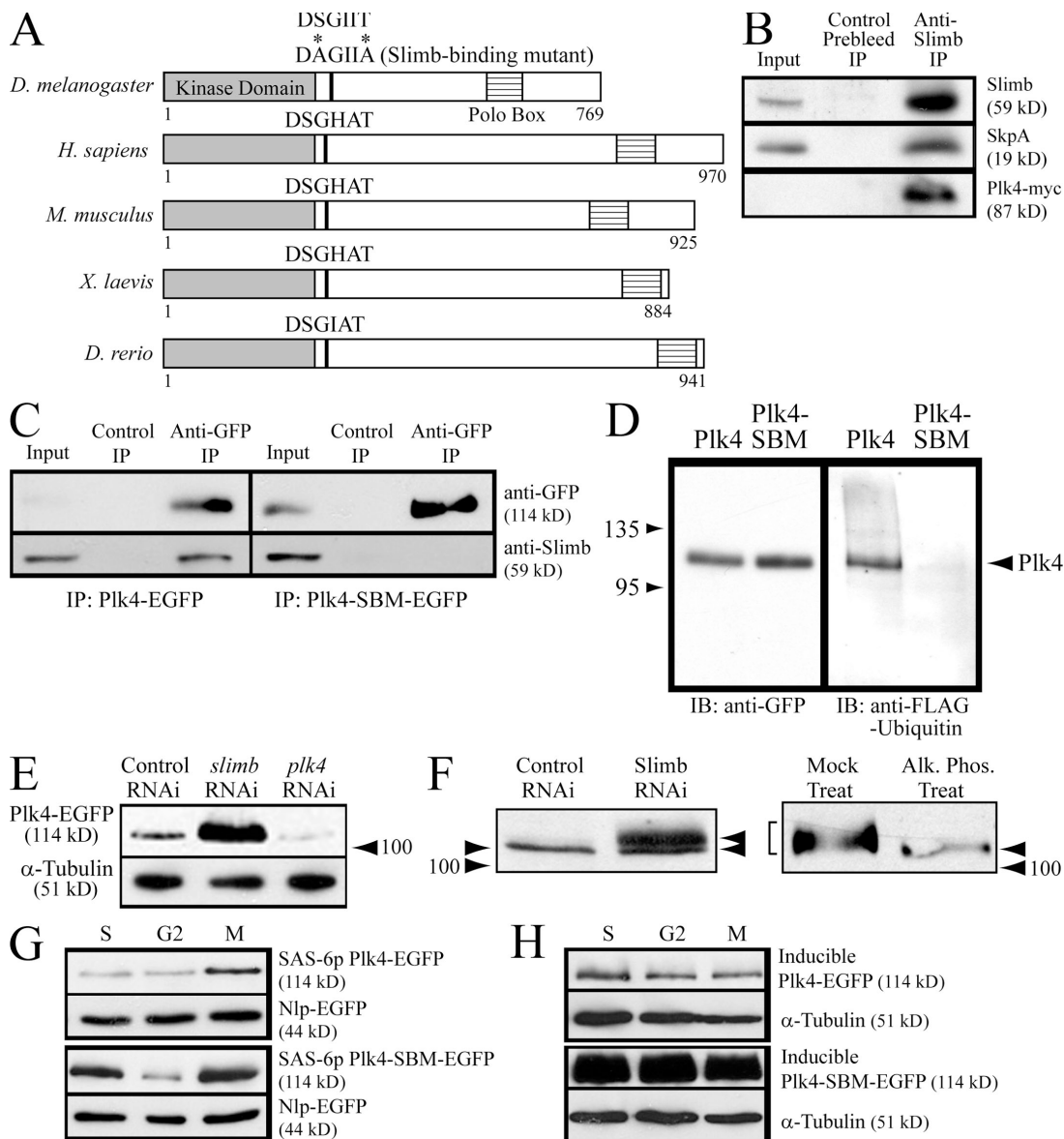


Figure 3. Plk4 is degraded in a Slimb-dependent manner and is stabilized by perturbing its interaction with Slimb. (A) Plk4 family showing the conserved kinase domain (gray), Polo box motif (striped boxes), and Slimb-binding consensus (black bars). The S293A/T297A SBM should be nondegradable. (B) Preimmune control and anti-Slimb immunoprecipitates from stable S2 cell lysates expressing Plk4-myc were probed for anti-Slimb, SkpA, and myc. (C) Control and anti-GFP immunoprecipitates from S2 cell lysates transiently expressing either inducible wild-type Plk4-EGFP or Plk4-SBM-EGFP were probed for endogenous Slimb. IP, immunoprecipitation. (D) Anti-GFP immunoprecipitates from S2 cell lysates transiently expressing triple Flag-ubiquitin and either inducible wild-type Plk4-EGFP or Plk4-SBM-EGFP were probed with anti-GFP (left) and anti-Flag (right) antibody. IB, immunoblot. (E) Anti-GFP immunoblots of lysates prepared from stable SAS-6p-driven Plk4-EGFP that were RNAi treated for the indicated protein for 7 d. (F) Plk4 is phosphorylated. (left) Anti-GFP immunoblots of lysates from control or Slimb-depleted cells transiently expressing inducible Plk4-EGFP. Plk4 accumulates as a doublet (arrowheads) after *slimb* RNAi. (right) Anti-GFP immunoprecipitates from day 4 Slimb-depleted cells transiently expressing inducible Plk4-EGFP were mock or alkaline phosphatase treated. Plk4 shifts from a broad band (bracket) to a faster migrating single polypeptide (arrowhead). (D–F) Molecular mass is indicated in kilodaltons. (G) Anti-GFP immunoblots showing the levels of transiently expressed SAS-6p-driven Plk4-EGFP and Plk4-SBM-EGFP in 24-h drug-induced cell cycle-arrested cells. Cotransfected Nlp-EGFP was used as a loading control. (H) Anti-GFP immunoblots showing the levels of 4 h-induced Plk4-EGFP and Plk4-SBM-EGFP expression in drug-induced cell cycle-arrested cells. (E and H) α-Tubulin was used as a loading control.

(Fig. 3 F, left). To test whether phosphorylation accounted for the slow migration of this new form of Plk4-EGFP, we immunoprecipitated Plk4-EGFP from Slimb-depleted cells and analyzed its migration in SDS-PAGE after alkaline phosphatase treatment. This shifted Plk4-EGFP back to the faster migrating species (Fig. 3 F, right). Thus, Slimb depletion stabilizes a phosphorylated form of Plk4. Although we cannot completely rule out an indirect role for Slimb in regulating Plk4 levels, collectively, our

results strongly suggest that Slimb binds and ubiquitinates a phosphorylated form of Plk4.

Based on these data, we hypothesized that Plk4 acts downstream of Slimb to regulate centriole duplication. If increased centriole number in Slimb-depleted cells requires Plk4, centriole number should not increase in double-depleted cells. We monitored Plk4 depletion by immunoblotting for GFP in a stable cell line expressing Plk4-EGFP under control of the weak

SAS-6 promoter (SAS-6p). Immunoblotting confirmed that *Plk4* RNAi reduced protein levels by 84%, whereas *slimb* RNAi produced massive *Plk4* accumulation (Fig. 3 E). *Plk4* depletion dramatically reduced centriole number (Figs. S1 C and S3 B) as previously described (Bettencourt-Dias et al., 2005). Codepletion of *Plk4* and *Slimb* also eliminated centrioles (Figs. S1 C and S3 B). Thus, *Plk4* is required for centriole reduplication in *Slimb*-depleted cells.

Plk4 levels on centrioles are high during mitosis and undetectable at S phase

Plk4 localizes to centrioles (Bettencourt-Dias et al., 2005). If *Plk4* regulates the timing of centriole duplication, its centriole localization should be tightly regulated through the cell cycle. To assess this, we drove *Plk4*-EGFP using the weak SAS-6p, which is expressed throughout the cell cycle (unpublished data). Because of its low expression, identifying *Plk4*-EGFP-transfected cells was made possible by cotransfected with the abundant nuclear protein nucleophosmin (Nlp)-EGFP (Ito et al., 1996). Notably, unlike mammalian Nlp, which localizes to centrosomes and suppresses their overduplication (Okuda et al., 2000; Wang et al., 2005), *Drosophila* Nlp does not localize to centrioles (Fig. S2 E), and *nlp* RNAi has no effect on centriole number (not depicted). We found that *Plk4*-EGFP was asymmetrically localized on D-PLP-labeled centrioles in interphase (Fig. 4 A), as seen in mammalian cells (Kleylein-Sohn et al., 2007). To assess whether *Plk4* centriole localization is cell cycle regulated, we coexpressed *Plk4*-EGFP and mCherry-SAS-6 in cells chemically arrested during S, G2, or M phase (Fig. 4, B and C). *Plk4* was undetectable in S phase–arrested cells, whereas levels on centrioles peaked during mitotic arrest (Fig. 4 C). *Plk4*-EGFP was observed on centrioles in some but not all cycling interphase cells (Fig. 4 A), a population presumably lost after prolonged interphase drug arrest. Thus, whereas *Slimb* localizes to centrioles during interphase, *Plk4* on centrioles peaks during mitosis, and it is not detected there during S phase. This is consistent with the hypothesis that *Slimb* on centrioles can destabilize *Plk4* during a period of the cell cycle when centriole duplication occurs.

The expression of mouse *Plk4* is cell cycle regulated (Fode et al., 1996), providing an additional mechanism for regulating its levels. Like mouse *Plk4*, fly *Plk4* mRNA is expressed during S phase and peaks during mitosis (as assessed by RT-PCR of S2 cells arrested during different cell cycle stages; Fig. S3 C). These data suggest that transcriptional regulation cannot fully account for the differences in centrosomal localization we observed. In our localization experiments, we expressed *Plk4* using SAS-6p, which is expressed at roughly equal levels throughout the cell cycle (unpublished data). We wanted to ensure that expression via SAS-6p did not artificially reduce *Plk4* levels to a point at which it might be subject to regulatory mechanisms that do not normally regulate endogenous *Plk4*. In fact, quantitative RT-PCR revealed that SAS-6p *Plk4*-EGFP mRNA was expressed at levels 10–20 times higher than that of endogenous mRNA (Fig. S3 D). However, these levels are not sufficient to alter centrosome number over time (Table I), in contrast to high level overexpression of *Plk4*, which increases centriole number in S2 cells (Bettencourt-Dias et al., 2005). In spite of

this somewhat elevated expression, *Plk4*-EGFP protein levels displayed a similar cell cycle profile as endogenous *Plk4* mRNA, with the highest levels during mitosis (Fig. 3 G). These data suggest that the regulation of protein stability and transcriptional regulation may both contribute to control *Plk4* levels.

If *Slimb* regulates *Plk4* protein levels, loss of *Slimb* regulation should stabilize *Plk4* protein throughout the cell cycle. To test this, we compared levels of *Plk4*-EGFP with that of *Plk4*-SBM-EGFP with a mutated *Slimb*-binding domain. *Plk4*-SBM-EGFP protein levels were higher than wild-type *Plk4*-GFP throughout the cell cycle whether we drove expression with the weak SAS-6p (Fig. 3 G and Fig. S3 E) or the strong metallothionein-inducible promoter (Fig. 3 H). With the weaker SAS-6p, we also noted a *Slimb*-independent decrease in *Plk4*-SBM-EGFP levels during G2 (Fig. 3 G), suggesting a possible second mechanism of down-regulating *Plk4* protein specifically during this cell cycle phase. These findings suggest that disrupting *Plk4*–*Slimb* interactions dramatically stabilizes *Plk4* protein during interphase.

SBM *Plk4* accumulates on centrioles throughout the cell cycle and promotes excess daughter centriole formation

Our data suggest the hypothesis that SCF^{Slimb} regulates *Plk4* levels on centrioles. To test this hypothesis, we expressed SAS-6p–driven *Plk4*-SBM-EGFP and monitored its localization on centrioles during S, G2, and M phases. After arresting cells, *Plk4*-SBM-EGFP robustly accumulated at centrioles during all cell cycle phases that we examined (Fig. 4 D), in striking contrast to wild-type *Plk4*-EGFP (Fig. 4 C). Thus, mutating the *Slimb*-binding site stabilizes *Plk4* on centrioles at cell cycle stages when it normally would be absent.

According to our hypothesis, *Slimb* can promote the local degradation of *Plk4* at centrioles. Thus, both proteins should colocalize on centrioles. To test this, we transiently expressed *Plk4*-SBM-EGFP and immunostained for both *Slimb* and D-PLP. We found that *Slimb* and *Plk4*-SBM target centrioles in interphase cells as expected and colocalize (Fig. 5 A). These results support a model whereby *Slimb* can bind and ubiquitinate *Plk4* directly on centrioles.

To test whether centrioles are required for the degradation of *Plk4*, we eliminated centrioles by *sas-6* RNAi in cells expressing *Plk4*-EGFP and examined global *Plk4* levels by Western blots. SAS-6 is an essential centriole component (Dammermann et al., 2004), and, previously, we have shown that *sas-6* RNAi eliminates centrioles in S2 cells (Rogers et al., 2008). Remarkably, although *Plk4*-EGFP is stabilized by *Slimb* depletion, *Plk4*-EGFP is not stabilized by *sas-6* RNAi, remaining at the same levels as it was in controls (Fig. 5 B). Thus, centrioles are not apparently required for *Plk4* down-regulation.

Our hypothesis suggests that *Slimb*-mediated destruction of *Plk4* is critical for limiting centriole duplication. One prediction of this is that a *Plk4* mutant that cannot be targeted by *Slimb* should drive centriole reduplication, increasing centriole number. To test this, we examined cycling cells expressing *Plk4*-SBM-EGFP. Strikingly, these cells steadily increased their interphase centriole number over a 5-d time course (as measured using D-PLP immunostaining), reaching a level double that of

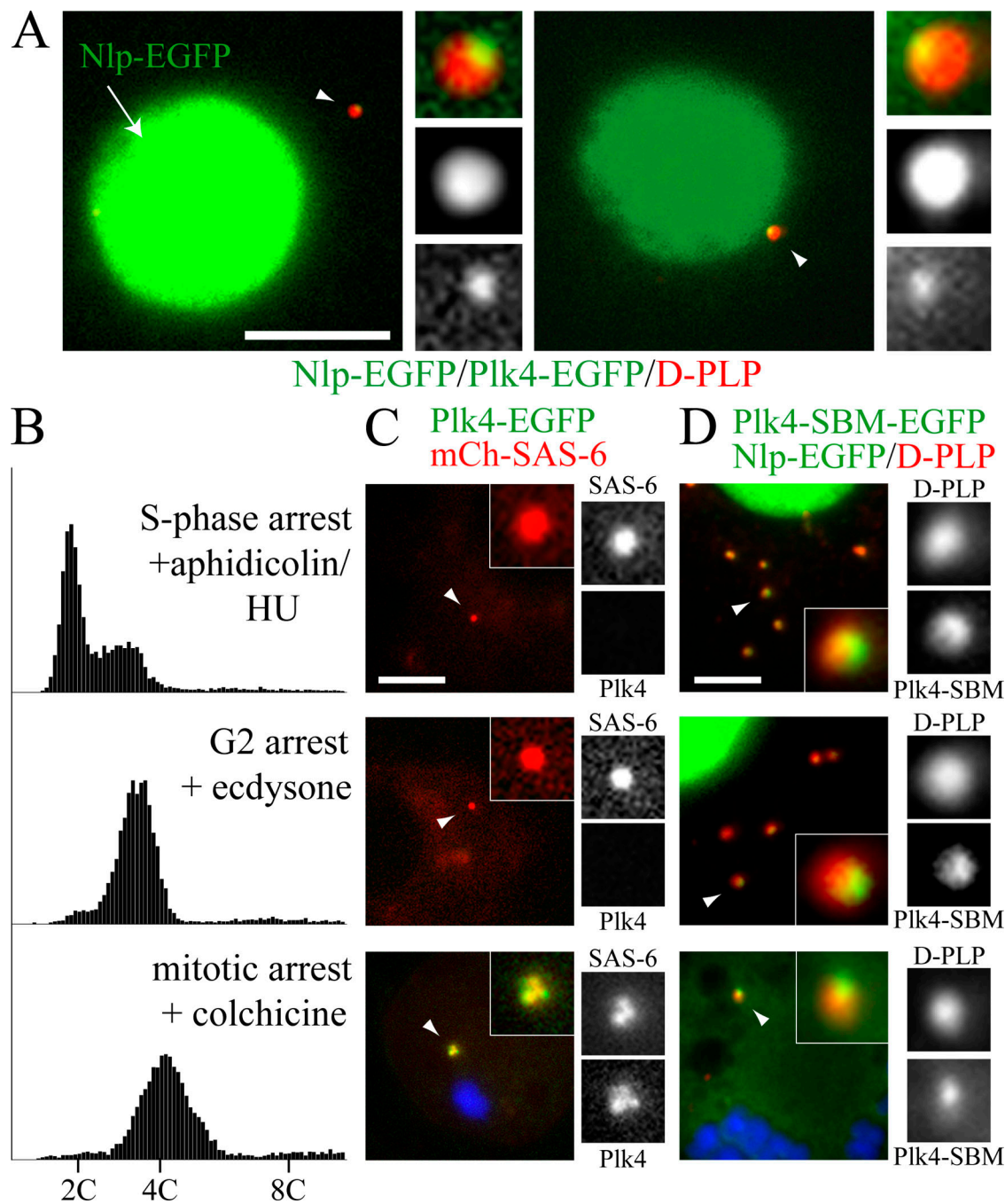


Figure 4. Slimb regulates Plk4 levels on centrioles to control centriole number. (A) Asymmetrical Plk4 localization. Transient cotransfection of Nlp-EGFP (Ito et al., 1996) as a cotransfection marker (green) labeling nuclei (arrow) and Plk4-EGFP (green). D-PLP (red) marks centrioles (arrowheads). Insets show centrioles at a higher magnification. (B–D) Mutating the Slimb-binding site stabilizes Plk4 on centrioles. (B) Cell cycle distributions after 24-h drug-induced S, G2, or mitotic arrest. Histograms are shown to scale and were assessed by HTM (5,000 cells/histogram). (C) Plk4-EGFP (green) only localizes to M-phase centrioles (arrowheads and insets) marked with mCherry-SAS-6 in live cells (red). Condensed DNA (blue) reveals mitotic cells. (D) Plk4-SBM-EGFP (green) localizes to centrioles during all cell cycle phases that were examined. Centrioles (arrowheads and insets) are marked with D-PLP in fixed cells (red). Nlp-EGFP (green nuclei, cytoplasmic during mitosis) is the cotransfection control. Bars: (A) 5 μ m; (C and D) 2.5 μ m.

wild type, whereas cells expressing Plk4-EGFP retained wild-type centriole numbers (Table I and Fig. 5, C and D). These data strongly support the hypothesis that Slimb acts through Plk4 to regulate centriole number.

Another interesting issue is how Plk4 promotes centriole duplication and how this is limited to once per cell cycle. Our imaging analysis provided insight into this mechanism. Cells

expressing Plk4-SBM-EGFP contained a mixed population of centrioles decorated with either one or two Plk4-SBM-EGFP spots (Fig. 5, A, C, and D), which is in contrast to wild-type Plk4-EGFP-expressing cells in which only one spot was seen (Fig. 4 A). The presence of multiple Plk4 centriole-associated spots in cells where Slimb–Plk4 interaction is perturbed suggested a mechanism underlying excess centriole duplication

Table I. Effects of wild-type Plk4 and SBM-Plk4 expression on centriole number

Day	Cycling cells ^a						S phase–arrested cells ^b					
	Plk4-EGFP			Plk4-SBM-EGFP			Plk4-EGFP			Plk4-SBM-EGFP		
	Total	Mean \pm SD	Median	Total	Mean \pm SD	Median	Total	Mean \pm SD	Median	Total	Mean \pm SD	Median
1	100	2.9 \pm 3.9	2.0	104	3.5 \pm 3.4	2.0	100	3.1 \pm 3.1	2.0	100	3.9 \pm 4.2	2.0
2	112	2.6 \pm 3.0	2.0	104	4.3 \pm 4.2 ^c	3.0	101	3.5 \pm 3.2	2.0	100	4.7 \pm 5.3	4.0
3	111	3.1 \pm 2.7	2.0	103	5.3 \pm 4.0 ^c	4.0	100	3.1 \pm 3.7	2.0	101	5.1 \pm 4.4 ^c	4.0
4	113	3.0 \pm 2.4	2.0	111	5.3 \pm 3.4 ^c	5.0	100	3.4 \pm 3.7	2.0	100	6.1 \pm 5.0 ^c	5.0
5	97	3.2 \pm 2.8	2.0	100	7.1 \pm 5.8 ^c	6.0	100	2.8 \pm 2.7	2.0	100	6.4 \pm 5.2 ^c	6.0

Expression of Plk4-EGFP and Plk4-SBM-EGFP was driven off of the weak SAS-6p. Positive transfected cells were identified by cotransfection with a plasmid expressing the nuclear protein Nlp-EGFP. Total, total cell number; mean and median columns refer to centriole number.

^aCentrioles were counted beginning 24 h after transfection.

^b24 h after transfection, cells were treated with aphidicolin/HU to arrest them through the time course of this experiment. Centrioles were quantified beginning 48 h after transfection.

^cIndicates a significant difference using an unpaired *t* test ($P < 0.001$).

whereby mother centrioles may assemble more than one daughter centriole at a time. Thus, we examined Plk4-SBM-EGFP-expressing cells by EM. Strikingly, we found examples of mother centrioles associated with two or more daughter centrioles (Fig. 5, E and F), which is something we never observed in wild type. Collectively, these data suggest that SCF^{Slmb} regulates Plk4 accumulation on centrioles in a cell cycle–dependent manner and that if Slmb recognition is perturbed, overduplication can occur by mother centrioles simultaneously assembling multiple daughter centrioles.

Slmb maintains an S-phase reduplication block by down-regulating Plk4 on centrioles

Normal cells can block centriole reduplication even after prolonged S-phase arrest, whereas some cancer cells lose the ability to block reduplication (Balczon et al., 1995; Wong and Stearns, 2003; Loncarek et al., 2008). The molecular mechanism remains unclear. We hypothesized that SCF^{Slmb} mediates this block by down-regulating Plk4. To test this, we treated S2 cells chemically arrested in S phase with RNAi and counted D-PLP centrioles over a 5-d time course (Table II). Control S2 cells possess a block to reduplication, as centriole numbers remained constant during the time course; *plk4* RNAi does not affect this block. However, after *slmb* RNAi, centriole numbers gradually increased over time. Plk4-EGFP was not present in S phase–arrested control RNAi–transfected cells where Slmb is active (Fig. 5 G, left) but was detected on centrioles in S phase–arrested cells treated with the proteasome inhibitor MG132 (Fig. 5 H). Strikingly, Plk4-EGFP reappeared on centrioles in Slmb-depleted S phase–arrested cells (Fig. 5 G, right). This also suggests that Slmb is not required for Plk4 to target centrioles. Thus, Slmb is required during S phase to block centriole number from increasing over time (Slmb might also affect separation of centriole pairs, as our visualization methods cannot distinguish centriole singlets and doublets; however, our aforementioned EM analysis suggests that if it does so, it also regulates duplication). Slmb depletion allows Plk4 accumulation on centrioles and abrogates this block.

As a final test, we examined whether Plk4 accumulation is necessary and sufficient to evade the S-phase block to centriole reduplication. Centriole number did not increase in cells co-

depleted of both Slmb and Plk4 (Table II), showing that Plk4 is necessary for evading the block (but not required to maintain centriole integrity during S-phase arrest). To test whether Plk4 accumulation at centrioles is sufficient for evading the S-phase block, we expressed Plk4-SBM-EGFP in S phase–arrested cells. Strikingly, median centriole number increased over time, reaching a level threefold higher than wild type (Table I). In contrast, centriole number was maintained at wild-type levels in cells expressing Plk4-EGFP (Table I). Thus, SCF^{Slmb} regulates Plk4 levels to maintain an S-phase block to centriole reduplication.

Discussion

Limiting centriole duplication to once and only once per cell cycle is a key event in all eukaryotes, ensuring that cells form a bipolar spindle and correctly segregate their chromosomes. Defects in this can cause genomic instability and may contribute to cancer. Despite more than a century of interest in this issue (Boveri, 1929) and despite advances in understanding the centrosome cycle (Tsou and Stearns, 2006b), mechanisms limiting centrosome duplication remain largely mysterious. In this study, we describe a mechanism accomplishing this goal, in which the SCF^{Slmb} ubiquitin ligase regulates stability of the key centrosome regulator Plk4, allowing it to stimulate centrosome duplication and then degrading it to prevent reduplication.

A novel mechanism for regulating centrosome duplication

One mechanism limiting DNA replication to once and only once per cell cycle involves E3 ubiquitin ligases that regulate stability of replication licensing factors. When we began, there were indications that several E3 ubiquitin ligases might also regulate centrosome duplication, as mutations in SkpA and the F-box proteins Slmb and Skp2 affect centrosome number (Wojcik et al., 2000; Nakayama et al., 2000; Guardavaccaro et al., 2003; Murphy, 2003). We comprehensively examined all identifiable fly Roc, Cullin, Skp, and F-box proteins using two different screens to sort out primary regulators of the centrosome cycle from those affecting cell cycle progression. The results were striking: SCF^{Slmb} plays a key role in regulating centriole number, as mutations in all subunits affect this. In contrast, none of

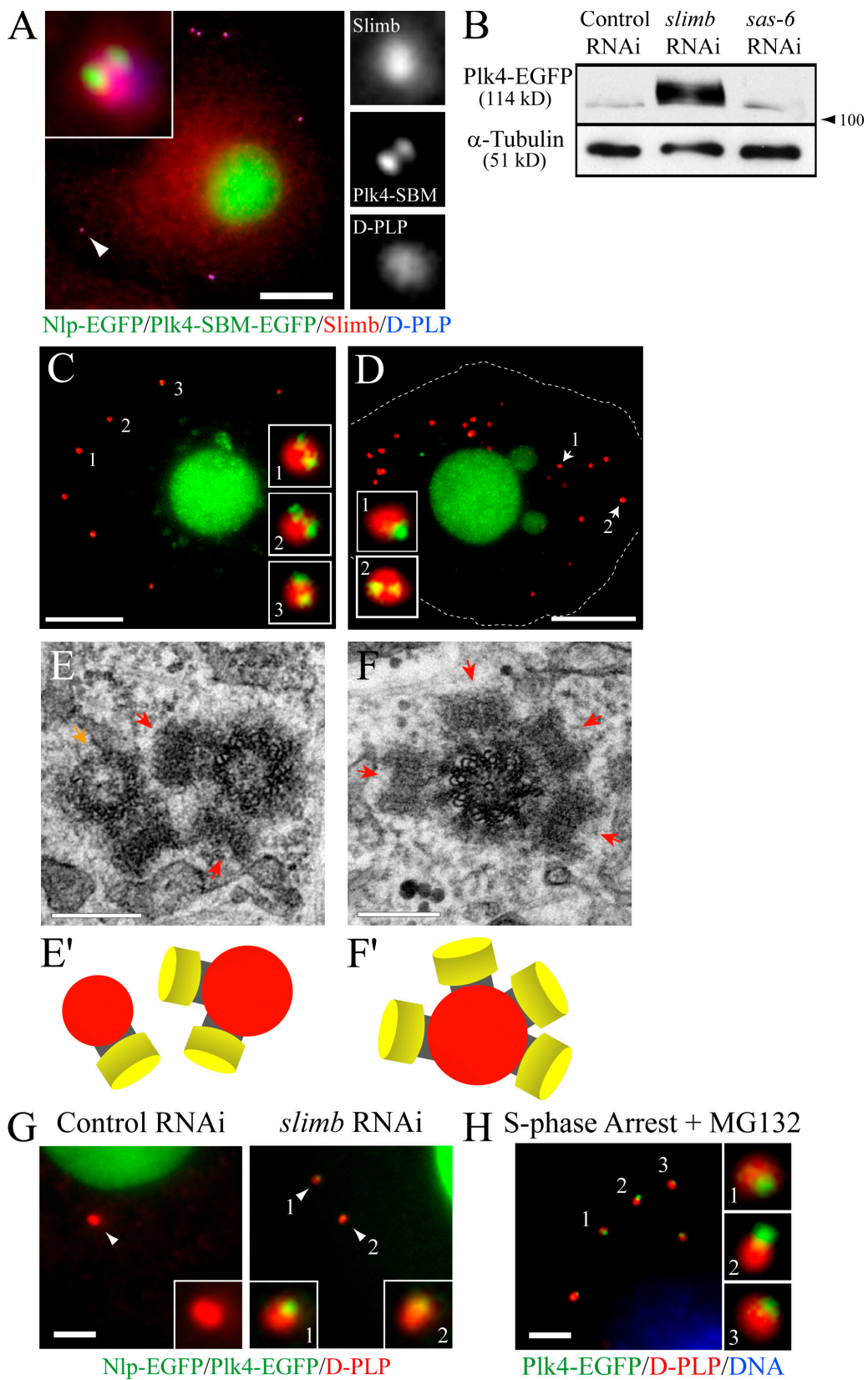


Figure 5. Stable Plk4 promotes excess daughter centriole formation, and *slimb* RNAi eliminates the S-phase centriole reduplication block by accumulating Plk4 on centrioles. (A) Slimb overlaps Plk4-SBM-EGFP localization on centrioles. Immunostaining of Slimb (red) and D-PLP centrioles (blue) in a transiently expressing coexpressing Nlp-EGFP (green nuclei) and SAS-6p Plk4-SBM-EGFP (green) interphase S2 cell. A representative centriole (arrowhead) is shown at a higher magnification (inset). (B) Anti-GFP immunoblots of lysates prepared from transiently expressing inducible Plk4-EGFP that were RNAi treated for the indicated proteins for 7 d. α -Tubulin was used as a loading control. Molecular mass is indicated in kilodaltons. (C and D) Transient coexpression of Nlp-EGFP (green nuclei) and Plk4-SBM-EGFP in day 5 cycling S2 cells. Plk4-SBM-EGFP labels one or more spots (green) on D-PLP-stained centrioles

Table II. Quantitation of centriole number in S phase–arrested RNAi-treated S2 cells

Day ^a	Control RNAi			slimb RNAi			plk4 RNAi			plk4/slimb RNAi		
	Total	Mean ± SD	Median	Total	Mean ± SD	Median	Total	Mean ± SD	Median	Total	Mean ± SD	Median
0	159	2.8 ± 3.0	2.0	173	3.2 ± 4.0	2.0	170	2.9 ± 3.5	2.0	171	2.8 ± 3.6	2.0
1	148	2.6 ± 2.9	2.0	169	3.0 ± 3.3	2.0	175	2.6 ± 2.9	2.0	172	2.5 ± 3.2	2.0
2	181	2.3 ± 2.1	2.0	169	2.8 ± 3.1	2.0	166	2.8 ± 3.2	2.0	186	2.7 ± 2.8	2.0
3	169	2.5 ± 2.5	2.0	179	3.4 ± 3.4 ^b	3.0	170	2.4 ± 2.5	2.0	171	2.9 ± 3.8	2.0
4	157	2.2 ± 2.3	2.0	157	3.9 ± 3.8 ^b	3.0	160	2.6 ± 2.9	2.0	160	2.4 ± 3.1	2.0
5	150	2.4 ± 2.2	2.0	126	4.4 ± 3.8 ^b	4.0	142	2.4 ± 4.0	2.0	154	2.3 ± 3.3	2.0

Total, total cell number; mean and median columns refer to centriole number.

^aCells were treated with 10 µg dsRNA, 10 µM aphidicolin, and 1.5 mM HU and processed for D-PLP immunofluorescence. This procedure was started on day 0 and repeated every 24 h.

^bIndicates a significant difference in the mean centriole value compared with the control population using an unpaired *t* test ($P < 0.003$).

the other proteins tested played a key role in regulating centrosome number under the conditions of our screen, with the exception of Skp2. Cells from Skp2-null mice display supernumerary centrosomes and an altered cell cycle geared toward DNA endoreduplication (Nakayama et al., 2000). In our screen, *skp2* RNAi did not affect interphase centriole number but increased mitotic centrosome number and induced endocycles (unpublished data). Thus, SCF^{Slmb} appears to be the sole identifiable Cullin-based ubiquitin ligase regulating centriole number; however, it is possible that roles for other F-box proteins are hidden by potential redundancy between different F-box proteins.

Given these data, we pursued the identity of the Slmb target, searching for candidate proteins with a Slmb-binding consensus. This led us to Plk4. Our data reveal a novel mechanism for limiting centriole duplication to once per cell cycle, suggesting a model in which Plk4 levels are regulated throughout the cell cycle by ubiquitin-mediated proteolysis via SCF^{Slmb} (Fig. 6). Throughout the cell cycle, the F-box protein Slmb resides on centrioles, which are primed to degrade Plk4. During mitosis, Plk4 localizes to centrioles, where it presumably phosphorylates an unknown centriole substrate required to initiate duplication later in the cell cycle. (We note that the levels of Slmb and Plk4 on centrioles have not been determined during G1 phase. In an asynchronous S2 population, however, anti-Slmb staining is detected on centrioles in every cell we have examined.) At some point after mitotic exit (likely during G1 phase), Plk4 levels fall as a result of SCF^{Slmb}-mediated proteolysis (this may occur throughout the cell or on centrioles). During S and G2 phases, Slmb on centrioles prevents Plk4 centriole accumulation and blocks reduplication. During the subsequent M phase, Plk4 levels rise and Plk4 reassociates with centrioles. Although both Slmb and Plk4 localize to mitotic centrioles, we hypothesize

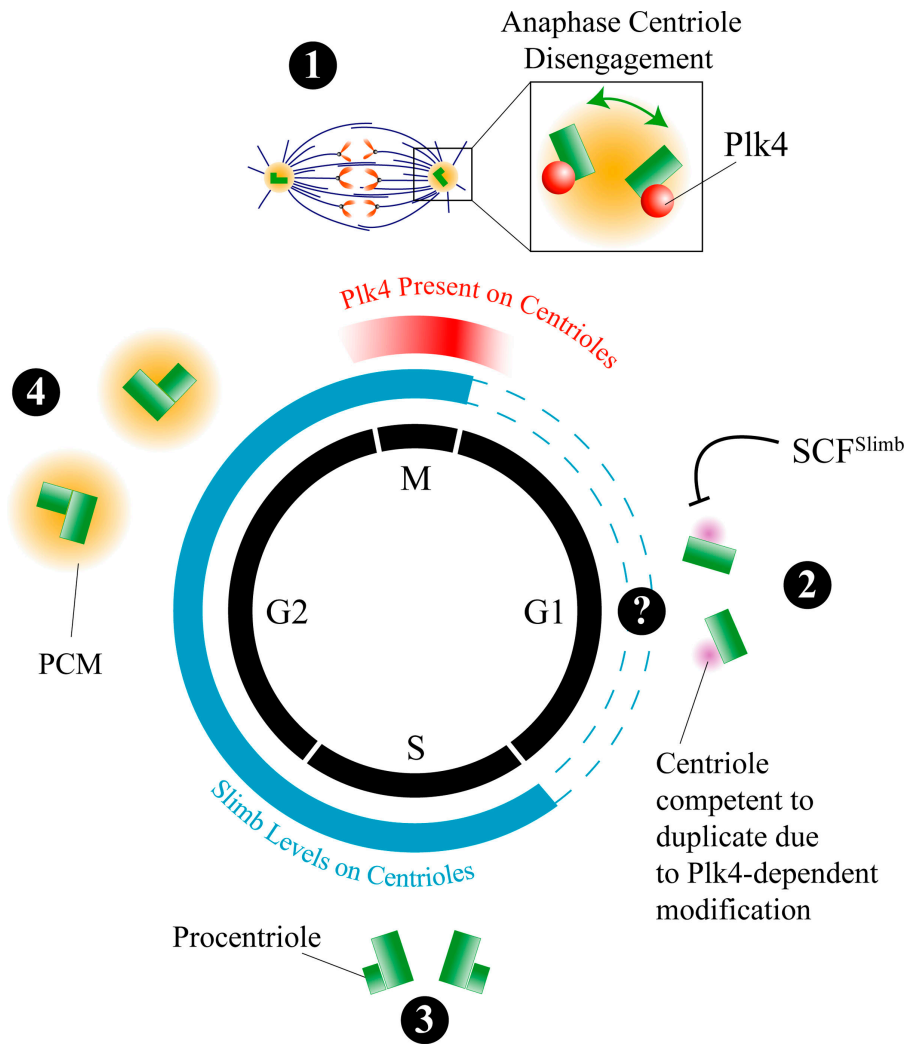
that one or more cell cycle–regulated kinases phosphorylate Plk4, priming it for recognition by SCF^{Slmb} at times other than during mitosis. This is consistent with the mechanisms by which SCF^{Slmb} recognizes other targets and consistent with the effect of our point mutations in two conserved serine/threonine residues in the Slmb-binding motif. It will be important to identify these kinases and determine how they are regulated, assessing phosphorylation and ubiquitination in vivo and in vitro. It will also be important to explore how Slmb recruitment to centrioles is regulated and whether this is dependent on Plk4 kinase activity.

Determining where Plk4 ubiquitination occurs is another important issue. Plk4 is a protein of low abundance and is only detected on centrioles, whereas Slmb is a relatively abundant cytoplasmic and nuclear protein that is also enriched on centrioles. Our hypothesis is that SCF^{Slmb} ubiquitinates a phosphorylated form of Plk4 directly on centrioles to control centriole duplication, although this need not be the case. We found that Plk4 is efficiently degraded when driven under a strong inducible promoter in cells that contain or lack centrioles. Therefore, it is likely that cytosolic SCF^{Slmb} can recognize and degrade Plk4 as long as the phosphorylation state of Plk4 permits this. Indeed, the ability of SCF^{Slmb} to globally promote Plk4 degradation may be crucial in suppressing de novo centriole assembly, a unique activity of Plk4 (Rodrigues-Martins et al., 2007). Thus, it will be important to determine the role of SCF^{Slmb} in regulating de novo centriole assembly, a phenomena that is poorly understood. Although centrioles appear dispensable for Plk4 degradation, these results do not negate the possibility that Slmb normally promotes the local degradation of Plk4 directly at centrioles.

This mechanism to prevent centriole reduplication may be conserved in mammals. Cells lacking β-Trcp1 (mammalian

(red)). Insets show select centrioles at a higher magnification. The cell in D shows an extreme example of centriole overduplication. White tracing marks cell borders. (E and F) Transmission electron micrographs of interphase cells expressing Plk4-SBM-EGFP for 5 d. Red arrows denote excess daughter centrioles emanating from mother centrioles shown in the cross section. The cell in E shows a normal mother–daughter centriole pair (orange arrow) adjacent to a mother with two daughters. Illustrations of these centrioles are shown in E' and F'. (G) Transient expression of Plk4-EGFP/Nlp-EGFP (green) in day 3 RNAi-treated cells arrested in S phase for 2 d. D-PLP–labeled centrioles (red, arrowheads). Insets show centrioles at a higher magnification. (H) Stable expression of Plk4-EGFP (green) in a 24-h S phase–arrested cell treated with MG132 proteasome inhibitor. Insets show select D-PLP–labeled centrioles (red) at a higher magnification. Bars: (A–D) 5 µm; (E and F) 0.2 µm; (G and H) 2.5 µm.

Figure 6. Speculative model for a mechanism to limit centriole duplication to once per cell cycle by modulating the levels of Plk4 on centrioles through the activity of the SCF^{Slmb} ubiquitin ligase. (1) Plk4 levels on centrioles peak during mitosis but also appear asymmetrically positioned on centrioles in a subpopulation of interphase cells. At this time, Plk4 activity initiates the duplication process by “priming” centrioles for the duplication event that occurs later in the cell cycle. This could be achieved by targeting or stabilizing a key centriolar subunit to the parent centriole that then lays the foundation to assemble a procentriole. During mitotic exit, centriole pairs separate (disengage), thereby releasing centriole singlets into the interphase cytoplasm (Callaini and Riparbelli, 1990). Although Slmb localizes to centrioles during all of the cell cycle phases that we examined, Plk4 is not phosphorylated on residues required for Slmb binding during mitosis and is thus stable. (2) As cells complete cytokinesis, centriole singlets shed their PCM and lack microtubule nucleating activity (Rogers et al., 2008). During interphase, Plk4 is phosphorylated and now recognized by SCF^{Slmb}, leading to its ubiquitination and degradation. Levels of centriole-associated Plk4 are low at this time. However, centrioles retain a critical modification (shown in purple) endowed upon them by Plk4 and are competent to duplicate. We note that Slmb and Plk4 levels on centrioles have not been determined during G1 phase. (3) Centrioles duplicate just before or during S phase with the appearance of a procentriole. Slmb on centrioles ensures that Plk4 levels remain low at this time and thus block centriole reduplication. (4) During G2, daughter centrioles elongate. Slmb at centrioles continues to prevent Plk4 accumulation.



Slmb) have excess centrosomes (Guardavaccaro et al., 2003). Human Plk4 is required for centriole duplication (Habedanck et al., 2005), and Plk4 overexpression produces mother centrioles associated with multiple daughters (Kleylein-Sohn et al., 2007), which is similar to the centriole configurations we observed by perturbing Slmb–Plk4 association. Moreover, inhibiting the proteasome in human cells also produces mother centrioles attached to multiple daughters (Duensing et al., 2007). It will be important to assess which features of our mechanism are conserved. Our proposed mechanism is different, but not mutually exclusive, from that described by Tsou and Stearns (2006b), who used an *in vitro* assay to identify a block to reduplication intrinsic to centriole conformation in which separation of centriole pairs during mitotic exit is required for S-phase duplication. We also note that we cannot rule out a separate role for Slmb in regulating centriole disengagement. Premature disengagement would also elevate apparent centriole number. It will be important in the future to examine this possibility.

Plk4 localizes asymmetrically on centrioles (Kleylein-Sohn et al., 2007), perhaps indicating a preferred binding site or nearby scaffold where Plk4 modifies its substrates (Rodrigues-Martins et al., 2007). We propose that during mitosis, Plk4 modifies and

primes centrioles for duplication later during S phase. Recent work analyzing centriole duplication after laser ablation of centrioles during S-phase arrest may support this hypothesis (Loncarek et al., 2008). After destruction of the daughter in a centriole pair, mother centrioles retained the ability to duplicate a new daughter. However, daughter centrioles could not duplicate after the destruction of their associated mother. Although there are other possible interpretations such as a role for PCM in centriole assembly (Loncarek et al., 2008), our priming model could also account for this difference. Mother centrioles would still possess the modification they received during the previous mitosis, allowing duplication. Laser ablating the daughter could expose this site, permitting duplication. However, because daughter centrioles have not yet received a Plk4 modification, duplication cannot occur after destruction of the mother.

Our data also suggest a possible molecular mechanism. Plk4 is asymmetrically localized on centrioles in both flies (our unpublished data) and mammals (Kleylein-Sohn et al., 2007), and this placement could define the site of daughter initiation. Furthermore, cells lacking Slmb sometimes had two spots of Plk4 on centrioles, and mothers were observed with multiple associated daughters. Perhaps Slmb helps limit Plk4 to a single high affinity site, ensuring that its putative substrate is also spatially

limited, resulting in the production of only a single daughter. An important goal will be to identify how Plk4 is targeted to centrioles and to identify its substrates there.

Possible parallels between centriole duplication and DNA replication are intriguing. Both occur once per cell cycle and are blocked from reinitiating by Cullin-based proteasomal targeting of critical regulators. Alterations or inactivation of the regulatory mechanism we describe may underlie the ability of some cells, like multiciliated cells, to increase centriole number, and misregulation of this pathway may also contribute to centrosome amplification and genomic instability during tumorigenesis.

Materials and methods

Cell culture and double-stranded RNAi

Drosophila S2 cell culture and RNAi were performed as described previously (Rogers and Rogers, 2008). Gene-specific primer sequences used to generate double-stranded RNA (dsRNA) are shown in Table S2 (available at <http://www.jcb.org/cgi/content/full/jcb.200808049/DC1>). In brief, cells were cultured in SF900II serum-free media (Invitrogen) without FBS. RNAi was conducted in 6-well plates, and cells (50–90% confluence) were treated with 10 µg dsRNA in 1 ml of media and replenished with fresh media/dsRNA every day for 7 d. Cell cycle arrest was induced by treating cells for at least 24 h with a final concentration of either 1 µM hydroxyurea (HU) + 10 µM aphidicolin (S phase), 1.7 µM 20-hydroxyecdysone (G2 phase), or 30 µM colchicine (mitosis). Colchicine treatment produces a mitotic index of ~20–30%, and, in some cases, Hoechst 33342 (Invitrogen) was added at a final concentration of 16.2 µM to identify mitotic cells containing condensed chromosomes. The cell cycle profiles in Figs. 2 F and 4 B are consistent with arrest at the stages indicated; HU/aphidicolin-arrested cells have a strong G1 peak and a small G2 peak, whereas ecdysone- and colchicine-arrested cells have a strong G2 peak. Cells were treated with 30 µM MG132 for 24 h.

RT-PCR

Total RNA was isolated from untransfected or SAS-6p Plk4-EGFP stable S2 cells using TRIZOL (Invitrogen). RNA was DNase treated for 30 min at 37°C followed by DNase inactivation for 10 min at 65°C. cDNA was generated from 1 µg of total RNA using standard conditions, and PCR was performed for Plk4 and Rp49 at 94°C for 30 s, 57°C for 30 s, and 72°C for 1 min. For semiquantitative RT-PCR, aliquots were removed at cycles 18, 20, 22, 24, 26, 28, and 30, and band intensity was determined using ImageJ software (National Institutes of Health). The following primers were used: Plk4 forward, 5'-ATAGAGCACGGAAACGAGTG-3'; Plk4 reverse, 5'-TGCCGAAGTGGGTTGAAG-3'; Rp49 forward, 5'-ATCCGCCAG-CATACAGG-3'; and Rp49 reverse, 5'-CTCGTTCTTGAGAACGCAG-3'.

Immunofluorescence microscopy

For immunostaining, S2 cells were fixed and processed exactly as described previously (Rogers and Rogers, 2008) by prespreading S2 cells on Con A-coated glass-bottom dishes and fixing with either cold methanol or formaldehyde (10% final). Antibodies used in this study were diluted to concentrations ranging from 1 to 20 µg/ml and include Slimb (provided by T. Murphy, Carnegie Institute of Washington, Baltimore, MD), SAS-6 and D-PLP (produced in our own laboratory; Rogers et al., 2008), α-tubulin DM1a (Sigma-Aldrich), γ-tubulin GTU-88 (Sigma-Aldrich), and phosphohistone H3 (Cell Signaling Technology). Secondary antibodies Cy2 and rhodamine red (Jackson ImmunoResearch Laboratories) were used at final dilutions of 1:100. Cells were mounted in a 0.1-M propyl gallate-glycerol solution. DAPI (Sigma-Aldrich) was used at a final concentration of 5 µg/ml. Specimens were imaged using a microscope (TE2000-E; Nikon).

Immunoblotting

S2 cell extracts were produced by resuspending cell pellets in PBS + 0.1% Triton X-100, and a small amount was removed to measure protein concentration. SDS-PAGE sample buffer was added and boiled for 5 min. The efficiency of RNAi was determined by Western blotting lysates in which equal protein amounts were loaded and bands were normalized using antibodies against α-tubulin. Antibodies used in this study were diluted to concentrations ranging from 1 to 20 µg/ml and include SkpA (provided by

T. Murphy), GFP JL-8 (Clontech Laboratories, Inc.), myc 9E10 (Developmental Studies Hybridoma Bank), Cullin-1 (Invitrogen), Cullin-4 (provided by S. Zacharek and Y. Xiong, University of North Carolina at Chapel Hill, Chapel Hill, NC), E2F1, Roc1a, Cullin-5 (provided by R. Duronio, University of North Carolina at Chapel Hill, Chapel Hill, NC), and Plk4 (provided by M. Bettencourt-Dias, Instituto Gulbenkian de Ciencia, Oeiras, Portugal). The percentage of depletion of the target protein was measured using the densitometry functions of ImageJ.

Antibody production

Escherichia coli-expressed GST- or maltose-binding protein-Slimb (amino acids 1–91) proteins were purified on either glutathione-Sepharose or amylose resin. Guinea pig polyclonal antisera (provided by T. Murphy) were raised against GST-tagged purified fusion protein, and the corresponding maltose-binding protein fusion was used for antibody affinity purification by precoupling to Affigel 10/15 (Bio-Rad Laboratories). Antibodies were affinity purified by elution with low pH buffer.

Immunoprecipitation

Polyclonal and monoclonal antisera were bound to equilibrated protein A- or protein G-Sepharose (Sigma-Aldrich), respectively, by gently rocking overnight at 4°C in 0.2 M sodium borate. In some cases, the prebound antibody was cross-linked to the resin using dimethyl pimelimidate by rocking for 1 h at 22°C, and the coupling reaction was quenched in 0.2 M ethanolamine, pH 8.0, by rocking for 2 h at 22°C. Antibody-coated beads were washed three times with 1.5 ml of cell lysis buffer (CLB; 50 mM Tris, pH 7.2, 125 mM NaCl, 2 mM DTT, 0.1% Triton X-100, and 0.1 mM PMSF). Transfected S2 cells were induced to express recombinant Plk4 with 350–500 mM CuSO₄ in the presence of 30 µM MG132. Cells were then lysed in CLB, precleared, and diluted to 2–5 mg/ml in CLB. Antibody-coated beads were mixed with lysate for 40 min at 4°C, washed three times with 1 ml CLB, and boiled in SDS-PAGE sample buffer. Alkaline phosphatase (New England Biolabs, Inc.) treatments were performed for 30 min at 37°C. In vivo ubiquitination assays were performed by coexpressing Plk4-EGFP constructs with triple Flag-tagged *Drosophila* ubiquitin (CG32744), driven under the fly actin (Act5) promoter, immunoprecipitated using anti-GFP antibody (Clontech Laboratories, Inc.), and analyzed by anti-Flag (Sigma-Aldrich) immunoblots.

Constructs and transfection

Endogenous promoters for GFP and mCherry constructs were made by PCR of genomic regions upstream of Slimb (960 bp), Nlp/CG7919 (429 bp; Ito et al., 1996), or SAS-6 (208 bp) and subcloned into pMT vectors (Invitrogen). Plk4-myc and Plk4-EGFP constructs were expressed either by the addition of 350 or 500 µM copper sulfate to the media to induce the metallothionein promoter or were under control of the low-expressing SAS-6p. QuikChange II (Agilent Technologies) was used to generate the Plk4 SBMs. Stable cell lines were generated using Effectene transfection reagent (QIAGEN) /pCoHygro selection system (Invitrogen). All stable cell lines expressing fluorescent proteins will be made available through the *Drosophila* Genomics Resource Center. Transient transfections were performed using the Nucleofector II (Amaxa) apparatus.

Live cell microscopy

S2 cells were plated on 0.5 mg/ml Con A-coated glass-bottom dishes (MatTek) for 1 h before observation. Cells were imaged with a 100x NA 1.45 Plan Apochromat objective using a microscope (TE2000-E) equipped with a cooled charge-coupled device camera (CoolSNAP HQ; Photometrics). Images were collected using MetaMorph software (MDS Analytical Technologies).

Centriole purification

Centrioles were purified exactly as described by Mitchison and Kirschner (1986).

Transmission EM

RNAi-treated S2 cells were plated as monolayers on Con A-treated polystyrene plates that were rinsed with PBS and fixed in 3% glutaraldehyde with 0.1 M sodium cacodylate, pH 7.4, for several hours or overnight. After buffer washes, the monolayers were postfixed for 1 h with 1% osmium tetroxide, 1.25% potassium ferrocyanide, and 0.1 M sodium cacodylate buffer. The cells were dehydrated using increasing concentrations of ethanol, infiltrated, and embedded in Polybed 812 epoxy resin (Polysciences, Inc.). The blocks were sectioned parallel to the substrate at 70 nm using a diamond knife, and the sections were mounted on 200 mesh copper grids followed by staining with 4% aqueous uranyl acetate and Reynolds' lead citrate. Sections were observed with a transmission electron microscope

(EM910; LEO Electron Microscopy) operating at 80 kV and photographed using a charge-coupled device digital camera (Orius SC1000; Gatan, Inc.) and Digital Micrograph 3.11.0 (Gatan, Inc.).

HTM

S2 cells were seeded in Con A-coated 24-well glass-bottom plates (Greiner) for 1 h before fixation, stained (as described in Immunofluorescence microscopy), and scanned with an Array Scan V (Cellomics) equipped with a 20x NA 0.5 or 40x NA 0.95 objective and a cooled charge-coupled device camera (ORCA-ER; Hamamatsu Photonics). Images of ~5,000 cells per well were acquired and analyzed using vHCS View (Cellomics). Integrated fluorescence intensity measurements were determined from unsaturated images.

Online supplemental material

Fig. S1 provides additional information regarding the Cullin-based RNAi screen performed in this study, which includes Western blots demonstrating the efficiency of RNAi, measurements of interphase centriole number, and frequencies of multipolar spindle formation. An illustration of the vertebrate canonical centrosome cycle is also shown to provide an introduction to the field of centrosome duplication. Fig. S2 provides additional phenotypic data of Slmb RNAi in S2 cells, which include distribution histograms of centriole number and Slmb immunostaining in RNAi-treated cells. A time series of S2 cell mitosis and several micrographs that show the centriole (and nuclear) markers used in the study are included. Fig. S3 shows additional data characterizing *Drosophila* Plk4 expression levels (both message and protein titers) as well as RNAi-induced phenotypes in S2 cells. Table S1 shows the results of the first Cullin-based RNAi screen performed in this study and lists the measurements of mitotic centrosome number in each RNAi treatment. Table S2 shows a list of all of the primer sequences used to generate the dsRNA templates in this study. Video 1 shows the colocalization of Slmb-GFP to a single centriole in a live S2 cell. Online supplemental material is available at <http://www.jcb.org/cgi/content/full/jcb.200808049/DC1>.

We thank R. Duronio, C. Jones, M. Bettencourt-Dias, K. Peters, E. Wagner, K. Slep, T. Murphy, and Y. Xiong for helpful comments and reagents.

This work was supported by a grant from the American Heart Association and National Institutes of Health grants RO1GM081645 to S.L. Rogers and RO1GM67236 to M. Peifer. N.M. Rusan was supported by American Cancer Society grant PF-06-108-01-CCC, and D.M. Roberts was supported by the National Institutes of Health National Research Service Award GM076898.

Submitted: 11 August 2008

Accepted: 19 December 2008

References

Balczon, R., L. Bao, W.E. Zimmer, K. Brown, R.P. Zinkowski, and B.R. Brinkley. 1995. Dissociation of centrosome replication events from cycles of DNA synthesis and mitotic division in hydroxyurea-arrested Chinese hamster ovary cells. *J. Cell Biol.* 130:105–115.

Bettencourt-Dias, M., A. Rodrigues-Martins, L. Carpenter, M. Riparbelli, L. Lehmann, M.K. Gatt, N. Carmo, F. Balloux, G. Callaini, and D.M. Glover. 2005. SAK/PLK4 is required for centriole duplication and flagella development. *Curr. Biol.* 15:2199–2207.

Blow, J.J., and A. Dutta. 2005. Preventing re-replication of chromosomal DNA. *Nat. Rev. Mol. Cell Biol.* 6:476–486.

Boveri, T. 1929. The Origin of Malignant Tumors. Williams and Wilkins Co., Baltimore, MD. 119 pp.

Brinkley, B.R. 2001. Managing the centrosome numbers game: from chaos to stability in cancer cell division. *Trends Cell Biol.* 11:18–21.

Callaini, G., and M.G. Riparbelli. 1990. Centriole and centrosome cycle in the early *Drosophila* embryo. *J. Cell Sci.* 97:539–543.

Dammermann, A., T. Muller-Reichert, L. Pelletier, B. Habermann, A. Desai, and K. Oegema. 2004. Centriole assembly requires both centriolar and pericentriolar material proteins. *Dev. Cell.* 7:815–829.

de Nooij, J.C., M.A. Letendre, and I.K. Hariharan. 1996. A cyclin-dependent kinase inhibitor, Dacapo, is necessary for timely exit from the cell cycle during *Drosophila* embryogenesis. *Cell.* 87:1237–1247.

DePamphilis, M.L., J.J. Blow, S. Ghosh, T. Saha, K. Noguchi, and A. Vassilev. 2006. Regulating the licensing of DNA replication origins in metazoa. *Curr. Opin. Cell Biol.* 18:231–239.

Deshaines, R.J. 1999. SCF and Cullin/Ring H2-based ubiquitin ligases. *Annu. Rev. Cell Dev. Biol.* 15:435–467.

Dimova, D.K., O. Stevaux, M.V. Frolov, and N.J. Dyson. 2003. Cell cycle-dependent and cell cycle-independent control of transcription by the *Drosophila* E2F/RB pathway. *Genes Dev.* 17:2308–2320.

Duensing, A., Y. Liu, S.A. Perdreau, J. Kleylein-Sohn, E.A. Nigg, and S. Duensing. 2007. Centriole overduplication through the concurrent formation of multiple daughter centrioles at single maternal templates. *Oncogene.* 26:6280–6288.

Fode, C., C. Binkert, and J.W. Dennis. 1996. Constitutive expression of murine Sak-a suppresses cell growth and induces multinucleation. *Mol. Cell. Biol.* 16:4665–4672.

Freed, E., K.R. Lacey, P. Huie, S.A. Lyapina, R.J. Deshaies, T. Stearns, and P.K. Jackson. 1999. Components of an SCF ubiquitin ligase localize to the centrosome and regulate the centrosome duplication cycle. *Genes Dev.* 13:2242–2257.

Guardavaccaro, D., Y. Kudo, J. Boulaire, M. Barchi, L. Busino, M. Donzelli, F. Margottin-Goguet, P.K. Jackson, L. Yamasaki, and M. Pagano. 2003. Control of meiotic and mitotic progression by the F box protein beta-Trep1 in vivo. *Dev. Cell.* 4:799–812.

Habedanck, R., Y. Stierhof, C.J. Wilkinson, and E.A. Nigg. 2005. The Polo kinase Plk4 functions in centriole duplication. *Nat. Cell Biol.* 7:1140–1146.

Hinchcliffe, E.H., G.O. Cassels, C.L. Rieder, and G. Sluder. 1998. The coordination of centrosome reproduction with nuclear events of the cell cycle in the sea urchin zygote. *J. Cell Biol.* 140:1417–1426.

Ito, T., J.K. Tyler, M. Bulger, R. Kobayashi, and J.T. Kadonaga. 1996. ATP-facilitated chromatin assembly with a nucleoplasm-like protein from *Drosophila melanogaster*. *J. Biol. Chem.* 271:25041–25048.

Kleylein-Sohn, J., J. Westendorf, M. Le Clech, R. Habedanck, Y.D. Stierhof, and E.A. Nigg. 2007. Plk4-induced centriole biogenesis in human cells. *Dev. Cell.* 13:190–202.

Ko, M.A., C.O. Rosario, J.W. Hudson, S. Kulkarni, A. Pollett, J.W. Dennis, and C.J. Swallow. 2005. Plk4 haploinsufficiency causes mitotic infidelity and carcinogenesis. *Nat. Genet.* 37:883–888.

Lane, M.E., K. Sauer, K. Wallace, Y.N. Jan, C.F. Lehner, and H. Vaessin. 1996. Dacapo, a cyclin-dependent kinase inhibitor, stops cell proliferation during *Drosophila* development. *Cell.* 87:1225–1235.

Loncarek, J., P. Hergert, V. Magidson, and A. Khodjakov. 2008. Control of daughter centriole formation by the pericentriolar material. *Nat. Cell Biol.* 10:322–328.

Martinez-Campos, M., R. Basto, J. Baker, M. Kernan, and J.W. Raff. 2004. The *Drosophila* pericentrin-like protein is essential for cilia/flagella function, but appears to be dispensable for mitosis. *J. Cell Biol.* 165:673–683.

Mitchison, T.J., and M.W. Kirschner. 1986. Isolation of mammalian centrosomes. *Methods Enzymol.* 134:261–268.

Murphy, T.D. 2003. *Drosophila* skpA, a component of SCF ubiquitin ligase, regulates centrosome duplication independently of cyclin E accumulation. *J. Cell Sci.* 116:2321–2332.

Nakayama, K., H. Nagahama, Y.A. Minamishima, M. Matsumoto, I. Nakamichi, K. Kitagawa, M. Shirane, R. Tsunematsu, T. Tsukiyama, N. Ishida, et al. 2000. Targeted disruption of Skp2 results in accumulation of cyclin E and p27 (Kip1), polyplody and centrosome overduplication. *EMBO J.* 19:2069–2081.

Nigg, E.A. 2006. Origins and consequences of centrosome aberrations in human cancers. *Int. J. Cancer.* 119:2717–2723.

Noureddine, M.A., T.D. Donaldson, S.A. Thacker, and R.J. Duronio. 2002. *Drosophila* Roc1a encodes a RING-H2 protein with a unique function in processing the Hh signal transducer Ci by the SCF E3 ubiquitin ligase. *Dev. Cell.* 2:757–770.

Okuda, M., H.F. Horn, P. Tarapore, Y. Tokuyama, A.G. Smulian, P.K. Chan, E.S. Knudsen, I.A. Hofmann, J.D. Snyder, K.E. Bove, et al. 2000. Nucleophosmin/B23 is a target of CDK2/cyclin E in centrosome duplication. *Cell.* 103:127–140.

Peel, N., N.R. Stevens, R. Basto, and J.W. Raff. 2007. Overexpressing centriole-replication proteins in vivo induces centriole overduplication and de novo formation. *Curr. Biol.* 17:834–843.

Rodrigues-Martins, A., M. Riparbelli, G. Callaini, D.M. Glover, and M. Bettencourt-Dias. 2007. Revisiting the role of the mother centriole in centriole biogenesis. *Science.* 316:1046–1050.

Rogers, G.C., N.M. Rusan, M. Peifer, and S.L. Rogers. 2008. A multi-component assembly pathway contributes to the formation of acentrosomal microtubule arrays in interphase *Drosophila* cells. *Mol. Biol. Cell.* 19:3163–3178.

Rogers, S.L., and G.C. Rogers. 2008. Culture of *Drosophila* S2 cells and their use for RNAi-mediated loss-of-function studies and immunofluorescence microscopy. *Nat. Protoc.* 3:606–611.

Rusan, N.M., and M. Peifer. 2007. A role for a novel centrosome cycle in asymmetric cell division. *J. Cell Biol.* 177:13–20.

Smelkinson, M.G., and D. Kalderon. 2006. Processing of the *Drosophila* hedgehog signaling effector Ci-155 to the repressor Ci-75 is mediated by direct binding to the SCF component Slimb. *Curr. Biol.* 16:110–116.

Tsou, M.F., and T. Stearns. 2006a. Controlling centrosome number: licenses and blocks. *Curr. Opin. Cell Biol.* 18:74–78.

Tsou, M.F., and T. Stearns. 2006b. Mechanism limiting centrosome duplication to once per cell cycle. *Nature*. 442:947–951.

Vodermaier, H.C. 2004. APC/C and SCF: controlling each other and the cell cycle. *Curr. Biol.* 14:R787–R796.

Wang, W., A. Budhu, M. Forques, and X.W. Wang. 2005. Temporal and spatial control of nucleophosmin in the RanA-Crm1 complex in centrosome duplication. *Nat. Cell Biol.* 7:823–830.

Winey, M. 1999. Cell cycle: driving the centrosome cycle. *Curr. Biol.* 9:R449–R452.

Wojcik, E.J., D.M. Glover, and T.S. Hays. 2000. The SCF ubiquitin ligase protein slimb regulates centrosome duplication in *Drosophila*. *Curr. Biol.* 10:1131–1134.

Wong, C., and T. Stearns. 2003. Centrosome number is controlled by a centrosome-intrinsic block to reduplication. *Nat. Cell Biol.* 5:539–544.

